Transient-estimate Monte Carlo in the two-dimensional electron gas

Yongkyung Kwon
Department of Physics, Kon-Kuk University, Seoul 133-701, Korea

D. M. Ceperley
Department of Physics and National Center for Supercomputing Applications, University of Illinois, Urbana, Illinois 61801

Richard M. Martin
Department of Physics and Materials Research Laboratory, University of Illinois, Urbana, Illinois 61801

(Received 28 July 1995)

Energies of the ground state and low-lying excited states of the two-dimensional electron gas have been calculated by a transient-estimate Monte Carlo method. This is an exact fermion quantum Monte Carlo method that systematically improves upon the results of a variational energy without imposing nodal constraints. We focus upon the density $r_s=1$, where our previous variational Monte Carlo calculation found qualitative differences in the effective mass from other theoretical approaches. Starting from a wave function with backflow and two-body correlations, the best trial function in our previous variational study, we find a ground-state energy only very slightly lower than the previously reported backflow fixed-node energy, reinforcing the conclusion that backflow wave functions are quite accurate. The effective mass derived from excitation energies does not differ significantly from the variational Monte Carlo results, giving a value of $m^*/m=0.93\pm0.01$, so we conclude that the effective mass is indeed less than bare electron mass for a range of densities around $r_s=1$.

I. INTRODUCTION

During the past three decades, the homogeneous two-dimensional (2D) electron gas, realized at interfaces of some semiconductor heterostructures, has attracted a great deal of interest among both theorists and experimentalists.[1] The pair correlation function and correlation energies of the 2D electron gas were calculated by Jonson,[2] using the dielectric function formalism. The contributions of the ring diagrams and the ladder diagrams to the ground-state energy have been computed independently by several authors.[3–5] Other approximate methods, such as one of using effective potential[6] and correlated-basis function approach,[7] have also been applied to investigate the ground-state properties of the system. Ceperley[8] first calculated, using Monte Carlo methods, upper bounds to the ground-state energy with trial functions consisting of the Slater determinant of single-body orbitals and products of two-body correlation functions. Tanatar and Ceperley,[9] using these trial functions, performed diffusion Monte Carlo (DMC) calculations. Even though the DMC method gives the exact ground-state energy for a system of many bosons, it was used within the fixed-node approximation[10] for the ground state of the fermionic many-body system. This approximation guarantees an upper bound to the true ground-state energy, which is usually much better than the variational one. One can systematically improve the results in quantum Monte Carlo (QMC) by using a better trial function.

Recently, we have reported DMC calculations of the ground-state properties of the 2D electron gas, using improved trial functions with backflow and three-body correlations, in addition to two-body correlation.[11] From the numerical results, we have provided an analytic expression for the correlation energy as a function of the density, which can be used to give exchange-correlation potential in density-functional calculations of inhomogeneous 2D electron systems. The compressibility measurement of Eisenstein *et al.*[12] is found to be in good qualitative agreement with the one calculated from our correlation energy.[13]

Following experimental work on the anomalous Landé g factor[14] and the effective mass m^* (Ref. 15) in the Si inversion layers, various approximate schemes[16–23] have been used to understand these phenomena microscopically. However, none of them could give quantitatively consistent results with the experiments. In a previous paper,[24] we have also applied the variational Monte Carlo (VMC) method to calculate low-lying particle-hole excitations of the 2D electron gas. As far as excited states are concerned, this was one of the few QMC calculations to date, among which are vibrational excited states of some molecules[25] and band gaps of model semiconductors[26,27] and solid hydrogen.[28] From the Fermi-liquid analysis[29] of the particle-hole excitation energies, we determined the many-body effective mass and other Fermi-liquid parameters. Our VMC calculations showed that the effective mass in the 2D electron gas is less than bare electron mass m over a wide range of high densities,[24] whereas other earlier analytic calculations produced the mass greater than m.[19–23] To confirm this result, here we shall go beyond the variational method.

In this work, we intend to examine how crucial the fixed-node approximation in our ground-state calculations is and how much our estimates of Fermi-liquid parameters obtained from the VMC calculations of the excitation energies depend on the trial wave functions used. For these purposes, here, we use a method, which can obtain, in principle, exact properties of both ground state and low-lying excited states. We

follow the approach proposed by Ceperley and Bernu,[30] which is a generalization of the transient-estimate method[31] used for fermion Green's function Monte Carlo. Actually, in this calculation, the energy differences are always between states of different momentum, so that a direct application of the transient-estimate method is possible.

II. METHODOLOGY

All properties of the electron gas without magnetic fields are determined only by the dimensionless density parameter $r_s = a/a_0$, where a_0 is the Bohr radius, $a = 1/\sqrt{\pi\rho}$ is the radius of a circle that encloses one electron on the average, and ρ is the number density. With energy units of Rydbergs (Ry) and the length units of a used here, the Hamiltonian of the electron gas is

$$H = -\frac{1}{r_s^2}\sum_{i=1}^{N}\nabla_i^2 + \frac{2}{r_s}\sum_{i<j}\frac{1}{|\mathbf{r}_i-\mathbf{r}_j|} + \text{const}, \tag{1}$$

where the const is the term due to the uniform background of opposite charge. Ewald sums[32] are used to calculate the long-range potential.

Let us suppose that the N-electron Hamiltonian H in Eq. (1) has eigenvalues E_i and eigenfunctions $\phi_i(\boldsymbol{R})$, where $\mathbf{R}=(\boldsymbol{r}_1,\boldsymbol{r}_2,\ldots,\boldsymbol{r}_N)$ is a $2N$-dimensional vector. We begin with applying a projection operator $C(H)=e^{-tH/2}$, where t is regarded as imaginary time, to a basis of known functions $\{f_i(\boldsymbol{R})\}$. Then, the eigenstate, which has the lowest energy and is not orthogonal to $f_i(R)$, dominates in the projected basis function $\tilde{f}_i(R)$ at large time t. As will be shown in Sec. III, we use a set of basis functions, which are not only orthogonal to each other, but are eigenfunctions of the total momentum, which commutes with the projection operator $C(H)$. Therefore, $\tilde{f}_i$'s are orthogonal to each other for all projection times t. The energy estimate of $\Lambda_i(t) = \boldsymbol{H}_{ii}(t)/\boldsymbol{N}_{ii}(t)$, where

$$\boldsymbol{N}_{ii}(t) = \langle\tilde{f}_i|\tilde{f}_i\rangle = \int d\boldsymbol{R}_1 d\,\mathbf{R}_2 f_i^*(\boldsymbol{R}_2)\langle\boldsymbol{R}_2|e^{-tH}|\mathbf{R}_1\rangle f_i(\boldsymbol{R}_1) \tag{2}$$

and

$$\boldsymbol{H}_{ii}(t) = \langle\tilde{f}_i|H|\tilde{f}_i\rangle = \int d\boldsymbol{R}_1 d\boldsymbol{R}_2 f_i^*(\boldsymbol{R}_2) \times\langle\boldsymbol{R}_2|He^{-tH}|\,\boldsymbol{R}_1\rangle f_i(\boldsymbol{R}_1) \tag{3}$$

is an upper bound to the true eigenvalue E_i for all t. Furthermore, $\Lambda_i(t)$ converges monotonically and exponentially fast to the exact energy eigenvalue E_i:

$$\lim_{t\to\infty}\Lambda_i(t) \to E_i + O[e^{-t(E_X-E_i)}], \tag{4}$$

where E_X is the energy of the next excited state with a nonzero overlap with the basis function f_i.

In order to calculate the multidimensional integrals $\boldsymbol{N}_{ii}(t)$ and $\mathrm{H}_{ii}(t)$, we will use diffusion Monte Carlo with the importance-sampled Green's function defined as

$$G(\boldsymbol{R}_2,\boldsymbol{R}_1;t) \equiv \Psi_G(\boldsymbol{R}_2)\langle\boldsymbol{R}_2|e^{-tH}|\boldsymbol{R}_1\rangle\Psi_G^{-1}(\boldsymbol{R}_1). \tag{5}$$

The *guiding function* Ψ_G, introduced to guide the random walks to important regions of phase space, must be positive everywhere the potential is finite, since the Green's function will be interpreted as a probability of moving a random walk from one place to another. A Green's function at time t can be rewritten as a path integral of k Green's functions at time argument $\tau = t/k$:

$$G(\boldsymbol{R}_k,\boldsymbol{R}_0;t) = \int d\boldsymbol{R}_1\cdots d\boldsymbol{R}_{k-1}\prod_{j=1}^{k} G(\boldsymbol{R}_j,\boldsymbol{R}_{j-1};\tau). \tag{6}$$

For a sufficiently small time interval τ, the Green's function can be approximated by

$$G(\boldsymbol{R}_2,\boldsymbol{R}_1;\tau) = G_b(\boldsymbol{R}_2,\boldsymbol{R}_1;\tau)G_d(\boldsymbol{R}_2,\boldsymbol{R}_1;\tau) \quad \text{as} \quad \tau\to 0, \tag{7}$$

where the branching term is

$$G_b(\boldsymbol{R}_2,\boldsymbol{R}_1;\tau) = e^{-\tau/2[E_{L\Psi}(\boldsymbol{R}_2)+E_{L\Psi}(\boldsymbol{R}_1)]}, \tag{8}$$

and the diffusion term is

$$G_d(\boldsymbol{R}_2,\boldsymbol{R}_1;\tau) = (4\pi D\tau)^{-N}e^{-[\boldsymbol{R}_2-\boldsymbol{R}_1-D\tau\boldsymbol{F}(\boldsymbol{R}_1)]^2/(4D\tau)}, \tag{9}$$

where $D = r_s^{-2}$, $E_{L\Psi}(\boldsymbol{R}) \equiv H\Psi_G(\,\mathrm{R})/\Psi_G(\boldsymbol{R})$ is the *local energy* of the guiding function, and $\boldsymbol{F}(\boldsymbol{R}) \equiv 2\Psi_G^{-1}(\boldsymbol{R})\boldsymbol{\nabla}\Psi_G(\boldsymbol{R})$ determines the drift velocity of the random walk.

Using this Green's function G, $\boldsymbol{N}_{ii}$, and $\boldsymbol{H}_{ii}$ can be rewritten as

$$\mathbf{N}_{ii}(t) = \int d\boldsymbol{R}_1 d\boldsymbol{R}_2 F_i^*(\boldsymbol{R}_2)G(\boldsymbol{R}_2,\boldsymbol{R}_1;t)F_i(\boldsymbol{R}_1)P(\boldsymbol{R}_1), \tag{10}$$

and

$$\mathbf{H}_{ii}(t) = \frac{1}{2}\int d\,\boldsymbol{R}_1 d\boldsymbol{R}_2 F_i^*(\boldsymbol{R}_2)\{E_{Li}^*(\boldsymbol{R}_2) + E_{Li}(\boldsymbol{R}_1)\}G(\boldsymbol{R}_2,\boldsymbol{R}_1;t)F_i(\boldsymbol{R}_1)P(\boldsymbol{R}_1), \tag{11}$$

where $F_i(\boldsymbol{R}) = f_i(\boldsymbol{R})/\Psi_G(\boldsymbol{R})$, $P(\boldsymbol{R}) = \Psi_G^2(\boldsymbol{R})$, and $E_{Li}(\boldsymbol{R}) = Hf_i(\boldsymbol{R})/f_i(\boldsymbol{R})$ is the local energy of a basis function $f_i(\boldsymbol{R})$.

Suppose that one constructs a trajectory $[\boldsymbol{R}_1,\boldsymbol{R}_2,\cdots,\boldsymbol{R}_p]$ by repeatedly sampling the diffusion Green's function $G_d(\mathbf{R}_{k+1},\boldsymbol{R}_k;\tau)$ with a small time step. We can estimate $\boldsymbol{N}_{ii}(k\tau)$ and $\boldsymbol{H}_{ii}(k\tau)$ by taking the averages over the trajectory[30] of the quantities

$$n_{ii}(k\tau) = F_i^*(\boldsymbol{R}_{n+k})W_{n,n+k}F_i(\boldsymbol{R}_n) \tag{12}$$

and

$$h_{ii}(k\tau) = \tfrac{1}{2}F_i^*(\boldsymbol{R}_{n+k})[E_{Li}^*(\boldsymbol{R}_{n+k}) + E_{Li}(\,\mathrm{R}_n)]W_{n,n+k}F_i(\boldsymbol{R}_n), \tag{13}$$

where the *weight* is defined as

$$W_{n,n+k}=\prod_{j=n}^{n+k-1} G_b(\boldsymbol{R}_{j+1},\boldsymbol{R}_j;\tau) \tag{14}$$

$$=\exp\left\{-\tau/2\sum_{j=n}^{n+k-1}[E_{L\Psi}(\boldsymbol{R}_j)+E_{L\Psi}(\boldsymbol{R}_{j+1})]\right\}. \tag{15}$$

Even though this method produces the exact eigenstates of quantum many-body systems, it has an intrinsic problem: as in the release-node methods for fermion ground states, its statistical error $\sigma_i(t)$ grows as the exponential of the difference between excited-state energy E_i and the absolute ground-state (i.e., Bose ground-state) energy E_0:[30]

$$\sigma_i(t)\propto\frac{e^{t(E_i-E_0)}}{N_c^{1/2}}, \tag{16}$$

where N_c is the number of configurations used. In order to get exact energy estimates, the projection must converge before the statistical errors get too large. That is the reason why this method is applicable only to low-lying excited states of systems with not too-many particles. Note that the total energies, E_i or E_0, are proportional to the number of particles. The method does produce smaller errors for the excitation energy, since the excited states and the ground state are estimated from the same trajectory.

We have done the transient-estimate calculations only at $r_s=1$, where our VMC effective masses with and without backflow correlation are almost indistinguishable and are less than the bare mass, unlike most of other previous analytic results.[24] Since there is a clear distinction between our VMC results and the previous values at $r_s=1$, it will suffice to consider only $r_s=1$ to establish the basic result that $m^*<m$ for a range of r_s much larger than in the previous analytic work and more like one sees in three dimensions. In addition to the computer time constraint, the fact that the statistical error in this method grows exponentially as the system size increases, requires us to do this calculation in the smallest size that we considered for the previous calculations, $N=26$.

As in Ref. 24, here we deal with the ground state and the lowest particle-hole excitations of the system. The ground state is considered as filled shells of the wave vectors allowed by periodic boundary conditions. We consider excited states, which consist of exciting a single electron from the last occupied shell of the ground state to the first unoccupied shell (see Fig. 1 of Ref. 24). The way we construct trial wave functions, either of the Slater-Jastrow or backflow type, is shown in Ref. 24. The goal of the present work is to obtain essentially exact energies for both the ground state and the low-lying excited states.

As in the VMC calculations,[24] we consider two different excitations, spin-parallel excitations and spin-antiparallel ones. The basis set $\{f_i(\boldsymbol{R})\}$ consists of the ground state and the spin-parallel excitations for one calculation and the spin-antiparallel excitations for the other. We use the following form for the guiding function:

$$\Psi_G^2(\boldsymbol{R})=a_0\Psi_0^2(\boldsymbol{R})+\sum_\alpha|\Psi_\alpha(\boldsymbol{R})|^2, \tag{17}$$

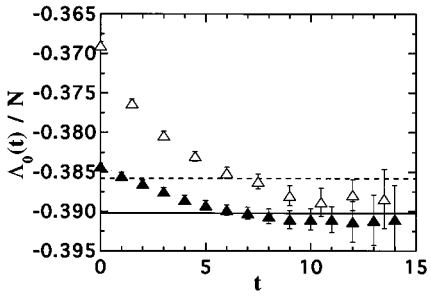

FIG. 1. The ground-state energies produced by the transient-estimate method with the Slater-Jastrow (open triangles) and backflow wave functions (filled triangles) vs the projection time. The calculation was done at $r_s=1$, for a system of 26 electrons. The energies are in units of Ry per electron and the imaginary-time unit is 0.02 Ry^{-1}. The dotted line and solid line show the Slater-Jastrow and backflow fixed-node energies obtained in Ref. 11, respectively. The error bars for the fixed-node energies are 0.0004 Ry for the Slater-Jastrow one and 0.0003 Ry for the backflow one.

where Ψ_0 is the trial function for the ground state, Ψ_α for excited state α. The constant a_0 is set to be equal to the number of excitations considered for spin-parallel excitations and to zero for spin-antiparallel excitations, as we discussed in Ref. 24. This guiding function is non-negative and zero only where all states under consideration have zeroes.

The properties of the guiding function are more important for the transient-estimate calculations than for the VMC calculations. This is because the weight of a random-walk trajectory defined in Eqs. (12)–(15) depends exponentially on the local energies of the guiding function $E_{L\Psi}(\boldsymbol{R})=H\Psi_G(\boldsymbol{R})/\Psi_G(\boldsymbol{R})$. Thus, fluctuations in $E_{L\Psi}(\boldsymbol{R})$ propagate exponentially into the statistical errors of the eigenvalue estimates $\Lambda_i(t)$. Difficulties arise especially if $E_{L\Psi}(\boldsymbol{R})$ is large and negative at a configuration R explored by the trajectory. This would occur where Ψ_G is small and has a large negative kinetic energy: $-\nabla^2\Psi_G$.

Ceperley and Alder[31] considered this point in their release-node calculations for the ground state, where they chose Ψ_G to be a bosonic ground-state function $\exp[-\Sigma_{i<j}^N u(r_{ij})]$. This avoids difficulties in the local energy, because the local energies are smooth and have little fluctuations in the configuration space. However, we find that this choice is not sufficient for our work, since it leads to large statistical errors even at the variational, or $t=0$, level without the weight factors. Even though the statistical errors could, in principle, be reduced with long runs, more efficient choices for Ψ_G are available.

We have instead used the guiding function Ψ_G in Eq. (17), which is close in magnitude to the variational fermion functions. This choice was found in Ref. 24 to greatly reduce the statistical fluctuations at the variational level; however, it leads to much larger fluctuations in the weights. In our calculations, we have found some cases where a trajectory acquires an extremely large weight $>2.2\times10^4$ times the average weight. This occurs in cases where Ψ_G becomes very small. In those cases, a single trajectory dominates over the entire finite set of trajectories, making the overall errors too large. We have avoided these points by simply rejecting trial moves in which $E_{L\Psi}$ would become too negative. A choice

of rejecting moves, with $E_{L\Psi}$ greater than 10 times its average value, led to good statistics for the transient-estimate energies. We do not believe that this cutoff causes significant bias, because the large weight occurs near the common nodal points of all states and should not be particularly relevant to the effective mass. However, this point needs to be further clarified in future work.

III. GROUND-STATE ENERGY

We first calculate the exact ground-state energy of the system and investigate how accurate our previous fixed-node calculations were at $r_s=1$. Since the ground state has zero total momentum, while the other states considered here have finite nonzero momenta, the energy estimate $\Lambda_0(t)$ is determined by the diagonal terms $\boldsymbol{H}_{00}(t)$ and $\boldsymbol{N}_{00}(t)$, as explained in the previous section. The open triangles of Fig. 1 show the ground-state energy $\Lambda_0(t)$ at projection time t obtained from the transient-estimate calculation with the Slater-Jastrow functions being used as basis functions. This was done for 7.3×10^6 steps with the time step $\tau=0.0005$ Ry^{-1}. The number of configurations averaged to compute the energy at projection time $k\tau$ is the number of steps minus k [see Eqs. (12) and (13)]. The unit of projection time in Fig. 1 and hereafter is 0.02 Ry^{-1} and the energy unit is Ry per electron. As expected, $\Lambda_0(0)$ is equal to the Slater-Jastrow variational energy in Ref. 11 within the statistical error. We see that the energy decreases as the projection time evolves. Around $t=6$, the transient-estimate energy is about the same as the Slater-Jastrow fixed-node energy of $-0.3858(4)$ Ry per electron, which was obtained from the finite-size scaling and the Slater-Jastrow fixed-node energy for $N=58$ in Ref. 11. Even though we get lower energies at larger times, the statistical errors grow too fast even before reaching the backflow fixed-node energy $-0.3902(3)$, which is the best upper bound to the true ground state known so far. In other words, the error is too large to determine the energy as accurately as the previous fixed-node DMC method.

With an improved basis function, we can start the simulation nearer the true ground state. This might enable us to get the converged energy, or the exact ground-state energy, from the transient-estimate calculation before the error becomes very large. The filled triangles of Fig. 1 show the ground-state energy produced with the backflow wave functions. The runs consisted of 3×10^6 steps and the time step used for each step or trial move was 0.001 Ry^{-1}. Here, we use the time step two times as big as in the Slater-Jastrow calculation, which is possible because the guiding function of Eq. (17) consisting of the backflow functions has smoother local energies. Once again, $\Lambda_0(0)$ corresponds to the (backflow) variational energy, which is far below the Slater-Jastrow variational value. The energy approaches the backflow fixed-node energy at $t=6$ and converges to $-0.3910(12)$ Ry per electron around $t=9$. This converged value is slightly below the backflow fixed-node energy, but the difference is on the order of the statistical error.

Table I summarizes the transient-estimate results for the ground state of a system of 26 electrons at $r_s=1$. The VMC and fixed-node DMC results shown in the table are from our previous calculations in Ref. 11. We set as t_1 the projection time where we can obtain the lowest energy estimate before the fast-growing statistical error kills our estimation. We have found in Fig. 1 that t_1 is 9×0.02 Ry^{-1} for both Slater-Jastrow and backflow calculations. $\Lambda_0(t_1)$ for the backflow calculation is almost the same as the corresponding fixed-node energy within the error, while for the Slater-Jastrow calculation, it is in the middle of the Slater-Jastrow and backflow fixed-node energy. We conclude, from these calculations, that our backflow fixed-node energy is within 10^{-3} Ry of the exact ground-state energy at the density $r_s=1$.

TABLE I. The results of the two transient-estimate calculations for the ground-state energy, using the Slater-Jastrow and backflow wave functions. The calculations were done at $r_s=1$, for a system of 26 electrons. The variational (VMC) and fixed-node diffusion Monte Carlo (FN-DMC) values were obtained from the finite-size scaling and the corresponding results for 58 electrons in Ref. 11. $\Lambda_0(t_1)$ represents the lowest energy estimate before the statistical error increases rapidly. The energies are in units of Ry per electron.

	Slater-Jastrow	Backflow
VMC	-0.3694(4)	-0.3839(4)
FN-DMC	-0.3858(4)	-0.3902(3)
$\Lambda_0(0)$	-0.3690(5)	-0.3843(5)
$\Lambda_0(t_1)$	-0.3880(13)	-0.3910(12)

IV. EXCITED STATES AND EFFECTIVE MASS

Now we turn to the particle-hole excitations. Following the Fermi-liquid analysis,[29] the energy difference between two excited states α and β is given by

$$\Delta E_{\alpha\beta}=\sum_{l=1}(f_l^s\pm f_l^a)[-\cos(l\theta_\alpha)+\cos(l\theta_\beta)], \qquad (18)$$

where $\theta_{\alpha(\beta)}$ is the angle between particle momentum $\boldsymbol{k}_p$ and hole momentum $\boldsymbol{k}_h$ in excitation $\alpha(\beta)$ and the $+(-)$ sign corresponds to parallel (antiparallel) spins between particle and hole. As explained in Ref. 24, the effective mass is determined by the first-order spin-symmetric component f_1^s:

$$\frac{m^*}{m}=(1-\tfrac{1}{4}r_s^2Nf_1^s)^{-1}. \qquad (19)$$

If we neglect higher than second-order terms in Eq. (18), it is sufficient for the effective mass to consider excitations 1 and 4 in Fig. 1 of Ref. 24, because f_1^s can be obtained by

$$Nf_1^s=\frac{N\Delta E_{14}^{\uparrow\uparrow}+N\Delta E_{14}^{\uparrow\downarrow}}{2(-\cos\theta_1+\cos\theta_4)}, \qquad (20)$$

where $\Delta E_{14}^{\uparrow\uparrow(\uparrow\downarrow)}$ is the energy difference between spin-parallel (-antiparallel) excitations 1 and 4. These excitations have different nonzero total momenta from each other, so that the excited-state wave functions, either Slater-Jastrow type or backflow type, serve as diagonal basis functions at an arbitrary projection time just like the ground-state functions in the previous section. Since spin-parallel excitations are considered along with the ground state, all spin-parallel results have been obtained from the same Monte Carlo trajectories as in the corresponding ground-state calculations.

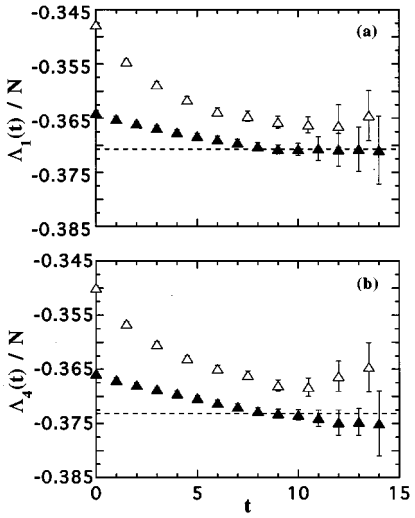

FIG. 2. Spin-parallel excitation energies produced by the transient-estimate method with the Slater-Jastrow (open triangles) and backflow functions (filled triangles) vs the projection time. (a) and (b) correspond to excitations 1 and 4 in Fig. 1 of Ref. 24, respectively. The dotted lines show the asymptotic values in the backflow calculations of each excitation energy.

Figure 2 shows the energies of spin-parallel excitations 1 and 4 at projection time t. From now on, the open triangles represent the results from the Slater-Jastrow transient-estimate calculations, while the filled triangles show the ones from the backflow calculations. Both $\Lambda_1(t)$ and $\Lambda_4(t)$ do not converge to asymptotic values in the Slater-Jastrow calculations before the statistical errors grow rapidly, as in the ground-state calculations of Fig. 1. The best estimation of the excited-state energies with reasonable error bars seems to occur at $t=9$, which is significantly higher than the converged energy from the backflow transient-estimate calculation. From Fig. 2(a), we clearly see that $\Lambda_1(t)$ converges to $-0.3707(8)$ Ry per electron at $t=9$ in the back-flow calculation. Even though it is less obvious, we conclude from Fig. 2(b) that $\Lambda_4(t)$ also reaches a converged value $-0.3731(8)$ Ry per electron at $t=9$. These converged excited-state energies are represented by the dotted lines.

The energy differences between the excitations depending on time t are shown in Fig. 3. The correlated sampling technique described in Ref. 24 is used here to reduce statistical fluctuations in the energy differences. The dotted line corresponds to the Slater-Jastrow variational value and the solid line to the backflow variational one from Ref. 24. It can be seen that the energy differences at $t=0$ in both Slater-Jastrow and backflow calculations are equal to the corresponding variational result within the error. Like each individual energy, we cannot see the convergence in the energy difference with Slater-Jastrow basis functions. With backflow basis functions, the energy differences hardly change from the (backflow) variational value until five units of the projection time.

The convergence problem with the Slater-Jastrow wave functions gets worse for calculation of spin-antiparallel excitations. Figure 4 shows the energies of spin-antiparallel excitations 1 and 4 at time t. In the Slater-Jastrow calculation,

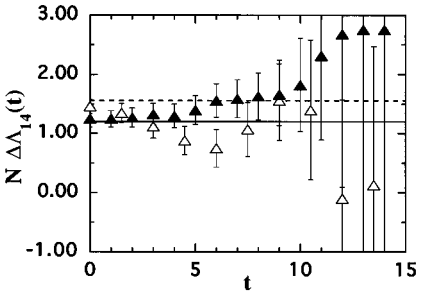

FIG. 3. The energy difference between two spin-parallel excitations 1 and 4 in Fig. 1 of Ref. 24 obtained by the transient-estimate method with the Slater-Jastrow (open triangles) and backflow basis functions (filled triangles) vs the projection time. The dotted and solid lines correspond to the Slater-Jastrow and backflow VMC energy differences of Ref. 24, respectively.

both excited-state energies keep decreasing, while the statistical errors grow rapidly especially after $t=6$. With the backflow functions, both $\Lambda_1(t)$ and $\Lambda_4(t)$ converge after $t_1=10$ time units. The dotted lines show the converged energies, $\Lambda_1(t_1)=-0.3733(10)$ and $\Lambda_4(t_1)=-0.3724(9)$ in units of Ry per electron, in the backflow calculations.

The energy differences $N\Delta\Lambda_{14}(t)$ between two spin-antiparallel excitations are plotted as a function of the time in Fig. 5. As in Fig. 3, the dotted and solid lines represent the Slater-Jastrow and backflow variational values,[24] respectively. We see that the energy difference with the Slater-Jastrow function is zero, which is the Slater-Jastrow variational value proved in Ref. 24, until a large statistical fluctuation makes the estimation meaningless. We did not include the Slater-Jastrow data at times $t>6$ in Fig. 5, because their fluctuations reach beyond the limit of this graph. The backflow calculations for the energy difference, shown

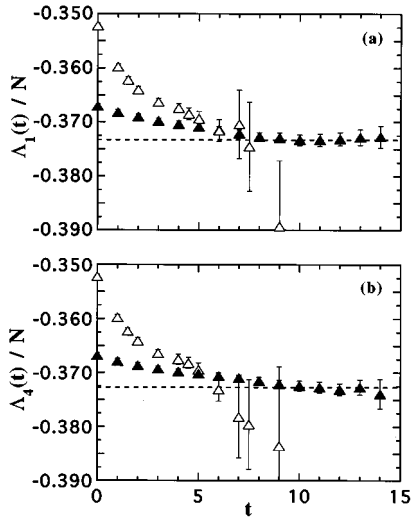

FIG. 4. Spin-antiparallel excitation energies produced by the transient-estimate method with the Slater-Jastrow (open triangles) and backflow basis functions (filled triangles) vs the projection time. The dotted lines show the asymptotic values in the backflow calculations of each excitation energy. (a) and (b) correspond to excitations 1 and 4 in Fig. 1 of Ref. 24, respectively.

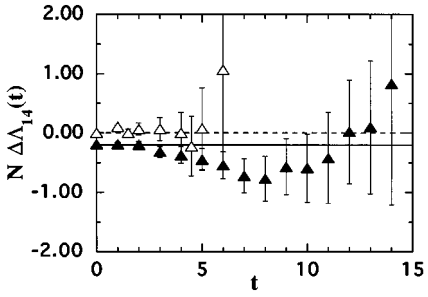

FIG. 5. The energy difference between two spin-antiparallel excitations 1 and 4 in Fig. 1 of Ref. 24 obtained by the transient-estimate method with the Slater-Jastrow (open triangles) and backflow basis functions (filled triangles) vs the projection time. The dotted line corresponds to the Slater-Jastrow variational value, which is zero as explained in Ref. 24. The solid line represents the backflow variational value in Ref. 24.

as the filled triangles, show very little difference from the corresponding variational result up to the convergence time $t_1=9$ for the individual excitations.

We have seen so far that the transient-estimate calculation of both spin-parallel and -antiparallel excitations with the Slater-Jastrow trial function does not converge before large statistical uncertainties make meaningful estimations impossible. The Slater-Jastrow trial functions are not accurate enough for this method to work. With the backflow function, we have found that the transient-estimate energies for the excited states converge well below the variational values before the statistical errors become large. However, the energy differences change very little, if any, up to the convergence times from the corresponding variational results. This implies that our effective mass obtained in Ref. 24 from the VMC calculations is correct, at least at $r_s=1$.

Since we have calculated the energy differences between excitations 1 and 4 as the projection time t evolves, we can estimate the effective mass through Eqs. (19) and (20) as a function of time t. This is plotted in Fig. 6. As can be seen,

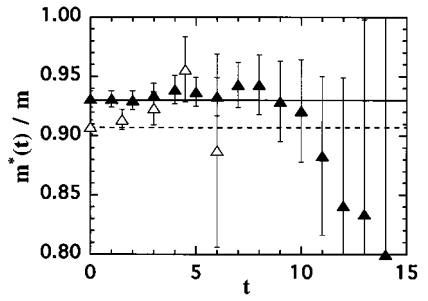

FIG. 6. The effective mass determined by the transient-estimate method vs the projection time. The filled triangles represent the backflow transient-estimate masses and the open triangles the Slater-Jastrow transient-estimate masses. The dotted line and solid line show the masses obtained by the VMC method with the Slater-Jastrow and backflow wave functions, respectively. The error bars for the VMC masses are 0.007 for Slater-Jastrow and 0.01 for backflow.

the Slater-Jastrow transient-estimate mass, denoted by the open triangles, increases toward the backflow VMC value until the errors explode at $t=6$. On the other hand, the backflow transient-estimate masses remain virtually equivalent to the backflow variational one until $t=9$, when the excited-state energies reach their asymptotic values (see Figs. 2 and 4). After that, the large statistical fluctuations dominate our estimation. We conclude from Fig. 6 that the effective mass obtained in Ref. 24 with the backflow VMC method, is confirmed to be accurate at $r_s=1$ by the transient-estimate calculations. This leaves the effective mass at $r_s=1$ less than m.

V. CONCLUSIONS

Transient-estimate calculations have been done at $r_s=1$ for 26 electrons, to get more accurate energies of both ground state and low-lying excited states without any approximation. We have used two different types of initial basis functions, Slater-Jastrow and backflow wave functions. The Slater-Jastrow calculations do not converge to the exact energies for both ground state and excited states before the error bars grow, because of the fermion sign problem. This reflects that the wave functions are relatively inaccurate and hence require a too large projection time to reach the true eigenstates.

With the backflow wave functions, we have found that the energies converge after a projection time of about 0.2 Ry^{-1} and the converged energy is in good agreement with the previous fixed-node calculation with an accuracy of 0.001 Ry/electron. This implies that the nodal surfaces of the backflow wave function are close enough to those of the exact ground-state wave function that the fixed-node method gives a very accurate energy at $r_s=1$. Future work should still check the accuracy at lower densities. The uncertainties of the exact ground-state energy might further be reduced by using the maximum entropy extrapolation of an imaginary-time correlation function $\boldsymbol{N}_{00}(t)$ in Eq. (2), the details of which are described in Ref. 33.

For particle-hole excitations shown in Fig. 1 of Ref. 24, the backflow transient-estimate calculations have also produced converged energy values at $r_s=1$, which are significantly below the corresponding variational energies. However, the energy differences between these excitations hardly change from the variational results. Thus, the effective mass computed from the energy differences is essentially unchanged from the backflow VMC calculations presented in Ref. 24 as being $m^*/m=0.93\pm0.01$. Even though these transient-estimate calculations are done only for 26 electrons, it was shown in Ref. 24 that our approach to determining the effective mass from the excited-state energy differences does not depend much on the system size. In other words, an accurate QMC calculation of the effective mass shows that it is less than the bare electron mass at $r_s=1$, unlike most of the previous results obtained with various analytic approximations.

In general, one expects $m^*<m$ for some range of small r_s in the high-density regime, because exchange dominates

over correlation at high density, giving an attractive interaction that decreases as a function of angle and a negative f_1^s parameter. Explicit high-density expansions in three dimensions show this behavior.[29] In fact, all the previous results in two dimensions either obviously show[23] or can be extrapolated to $m^*<m$ at very small r_s. The difference here is that the density range of $m^*<m$ found in our 2D QMC calculations is greater than that found in the other theoretical approaches. It more closely resembles Rice's results[34] for the 3D electron gas.

ACKNOWLEDGMENTS

We would like to thank G. Ortiz, G. Engel, and V. Rao for helpful discussions. This work has been supported by the Department of Energy under Contract No. DEFG 02-91-ER45439 and the National Science Foundation under Grant No. NSF DMR 91-17822. Y. Kwon acknowledges partial support from Kon-Kuk University under its 1995 research grant. The calculations were performed on the CRAY YMP at the National Center for Supercomputing Applications and IBM RISC/6000 workstations in the Materials Research Laboratory at the University of Illinois.

[1] T. Ando, A. Fowler, and F. Stern, Rev. Mod. Phys. **54**, 437 (1982); A. Isihara, in *Solid State Physics: Advances in Research and Applications*, edited by F. Seitz and D. Turnbull (Academic, New York, 1989). Vol. 42, p. 271.

[2] M. Jonson, J. Phys. C **9**, 3055 (1976).

[3] A. K. Rajagopal and J. C. Kimball, Phys. Rev. B **15**, 2819 (1977).

[4] A. Isihara and J. L. C. Ioriatti, Phys. Rev. B **22**, 214 (1980).

[5] D. L. Freeman, J. Phys. C **16**, 711 (1983).

[6] Y. Takada, Phys. Rev. B **30**, 3882 (1984).

[7] H. K. Sim, R. Tao, and F. Y. Wu, Phys. Rev. B **34**, 7123 (1986).

[8] D. M. Ceperley, Phys. Rev. B **18**, 3126 (1978).

[9] B. Tanatar and D. M. Ceperley, Phys. Rev. B **39**, 5005 (1989).

[10] P. J. Reynolds, D. M. Ceperley, B. J. Alder, and J. W. A. Lester, J. Chem. Phys. **77**, 5593 (1982).

[11] Y. Kwon, D. M. Ceperley, and R. M. Martin, Phys. Rev. B **48**, 12 037 (1993).

[12] J. P. Eisenstein, L. N. Pfeiffer, and K. W. West, Phys. Rev. Lett. **68**, 674 (1992).

[13] Y. Kwon, Ph.D. thesis, University of Illinois at Urbana-Champaign, 1994.

[14] F. F. Fang and P. J. Stiles, Phys. Rev. **174**, 823 (1968).

[15] J. L. Smith and P. J. Stiles, Phys. Rev. Lett. **29**, 102 (1972).

[16] J. F. Janak, Phys. Rev. **178**, 1416 (1969).

[17] K. Suzuki and Y. Kawamoto, J. Phys. Soc. Jpn. **35**, 1456 (1973); T. Ando and Y. Uemura, *ibid.* **37**, 1044 (1974).

[18] C. S. Ting, T. K. Lee, and J. J. Quinn, Phys. Rev. Lett. **34**, 870 (1975); T. K. Lee, C. S. Ting, and J. J. Quinn, *ibid.* **35**, 1048 (1975).

[19] T. K. Lee, C. S. Ting, and J. J. Quinn, Surf. Sci. **58**, 246 (1976).

[20] B. Vinter, Phys. Rev. Lett. **35**, 1044 (1975); Phys. Rev. B **13**, 4447 (1976).

[21] S. Yarlagadda and G. F. Giuliani, Phys. Rev. B **38**, 10 966 (1988); Surf. Sci. **229**, 410 (1990).

[22] G. E. Santoro and G. F. Giuliani, Solid State Commun. **67**, 681 (1988); Phys. Rev. B **39**, 12 818 (1989).

[23] Y. -R. Jang and B. I. Min, Phys. Rev. B **48**, 1914 (1993).

[24] Y. Kwon, D. M. Ceperley, and R. M. Martin, Phys. Rev. B **50**, 1684 (1994).

[25] B. Bernu, D. M. Ceperley, and J. W. A. Lester, J. Chem. Phys. **93**, 552 (1990).

[26] W. Knorr and R. W. Godby, Phys. Rev. Lett. **68**, 639 (1992).

[27] G. Engel, Y. Kwon, and R. M. Martin, Phys. Rev. B **51**, 13 538 (1995).

[28] D. M. Ceperley and B. J. Alder, Phys. Rev. B **36**, 2092 (1987).

[29] D. Pines and P. Nozières, *The Theory of Quantum Liquids* (Addison-Wesley, Reading, MA, 1989), Vol. 1.

[30] D. M. Ceperley and B. Bernu, J. Chem. Phys. **89**, 6316 (1988)

[31] D. M. Ceperley and B. J. Alder, J. Chem. Phys. **81**, 5833 (1984).

[32] P. Ewald, Ann. Phys. **64**, 253 (1921).

[33] M. Caffarel and D. M. Ceperley, J. Chem. Phys. **97**, 8415 (1992).

[34] T. M. Rice, Ann. Phys. **31**, 100 (1965).